Effects of a thin nitrogen-doped layer on terahertz dynamics in GaAs containing InAs quantum dots

Kojima, Osamu
Izumi, Ryo
Kita, Takashi

(Citation)
OSA Continuum,2(5):1621-1628

(Issue Date)
2019-05-15

(Resource Type)
journal article

(Version)
Version of Record

Research Article Vol. 2, No. 5 / 15 May 2019 / OSA Continuum 1621

Effects of a thin nitrogen-doped layer on terahertz dynamics in GaAs containing InAs quantum dots

OSAMU KOJIMA,* RYO IZUMI, AND TAKASHI KITA

Department of Electrical and Electronic Engineering, Graduate School of Engineering, Kobe University, 1-1 Rokkodai, Nada, Kobe 657-8501, Japan
kojima@phoenix.kobe-u.ac.jp

Abstract: The transient terahertz signal generated by electron diffusion that was excited by an ultrashort pulse was observed to vary with the potential structure around the surface. The formation of InAs quantum dots caused the strain field and the nitrogen atoms to further modify the potential structure around the quantum dots. The terahertz signal that was observed for various pump energies exhibited an interesting phase change. Further, the change in terahertz dynamics originated from the formation of a dilute nitrogen layer around the quantum dots. Furthermore, this change depends on the position of the nitrogen-doped layer. The results of this study provide important information for controlling the optical properties of quantum dots.

1. Introduction

Control of the optical properties of self-assembled quantum dots (QDs) is essential for device applications such as in lasers [1–3], single photon sources [4–6], and solar cells [7–9]. The control of strain [10–12] and intermixing of Ga and In [13–15] in case of InAs QDs on GaAs have been reported as methods to control the QD characteristics. Previously, covering the InAs QDs with nitrogen atoms has been reported as one of the control methods [16–21]. By covering the InAs QDs with nitrogen atoms, the photoluminescence (PL) energy decreases because of the strain relief; further, the PL intensity decreases because of an increase in the non-radiative recombination center. Furthermore, these are recovered by the insertion of a GaAs spacer; the PL energy and intensity increases.

On the other hand, the carrier dynamics can provide abundant information regarding the device efficiency. When the dynamics around the semiconductor surface is focused, the observation of the terahertz (THz) wave emitted from the surface can be considered to be a good tool. For instance, the direction of the surface depletion can be identified as the initial phase of the THz wave [22–25]. Recently, we reported the phase inversion of a THz wave emitted from a GaAs crystal that included InAs QDs, which was attributed to the lattice-mismatched strain [26]. As mentioned above, the effect of strain can be controlled by covering the QDs using nitrogen atoms, which realize the PL emission at 1.3-μm optical communication band at room temperature [16]. Actually, the nitrogen atoms act as the non-radiative center, this method may not be good for the luminescent devices. However, ultrafast optical switches require the ultrashort lifetime. Therefore, the covering QDs by the nitrogen atom can be good method for the ultrafast optical communication application. Furthermore, in addition to the strain, the optical properties of QDs are also modified during the growth of capping layer, because of In segregation into the capping layer. This In segregation, which is difficult to control, causes the size reduction and In-Ga intermixing. Therefore, understanding the potential structure modified by the change in the strain and In segregation caused by the nitrogen layer is significant to achieve the efficient device operation. Considering the traditional methods to know the exciton/carrier dynamics, such as the PL-decay profile which is basically obtained at the lowest emission state after the

#357972 https://doi.org/10.1364/OSAC.2.001621
Journal © 2019 Received 16 Jan 2019; revised 6 Apr 2019; accepted 6 Apr 2019; published 19 Apr 2019

OSA CONTINUUM

intraband relaxation and the pump-probe signal which is measured at the resonant state, the THz signal can give the information of the direction of the carrier diffusion, which is the advantage to measure the THz signal. Therefore, in this study, we discuss the effect of using a nitrogen layer to cover QDs on the time-domain THz signal. By covering the QDs, the strain effect changed because phase inversion occurred at different pump photon energies. Interestingly, although the PL intensity can be recovered by the insertion of a GaAs spacer layer between the QDs and the nitrogen layer, the photon energy for the phase inversion is observed to be different; the band lineup in the sample that contains the spacer layer is not the same as that in the simple QD sample. The variation of the THz signals is discussed from the aspect of the effects of the formation of a thin nitrogen-doped layer.

2. Experiments

The samples used in this study were self-assembled InAs QDs covered by nitrogen atoms with or without a GaAs spacer layer grown on a GaAs(001) substrate by solid-source molecular-beam epitaxy. The sample image is shown in Fig. 1. The spacer thickness was 5 nm. A sample without the nitrogen layer was used as the reference. The details of the samples have been explained in our previous reports [20,26,27]. InAs was deposited at a growth rate of 0.012 ML/s after growing a 500-nm buffer layer of GaAs at 550°C. The deposited InAs layer thickness was 3.6 ML. The average lateral QD length is 40 nm, and the QD density is approximately 1.45×10^{10} cm^{-2}. The deposition rate was estimated from the reflection high-energy electron diffraction oscillations during the homoepitaxial growth. Active nitrogen species were created in a radio-frequency (RF) plasma source from ultra-pure N_2 gas. The N_2 partial pressure was 5.0×10^{-5} Torr, and the gas-flow rate was 0.34 ccm. The RF power was set at 200 W. All the QDs were capped with a 150-nm thick GaAs layer. Hereafter, the three samples are referred to as NQD, NQD(5 nm), and reference QD. It is noted that the QDs are directly covered by nitrogen atoms only in NQD. Summarizing the difference in the QD properties by the previously observed PL properties, covering the QDs with nitrogen atoms generates non-radiative centers, which cause a weak PL intensity, while the nitrogen atoms relieve the strain. Insertion of a GaAs spacer layer cancels these effects; a decrease in the non-radiative centers increases the PL intensity, and the lattice-mismatched strain increases the PL peak energy [27].

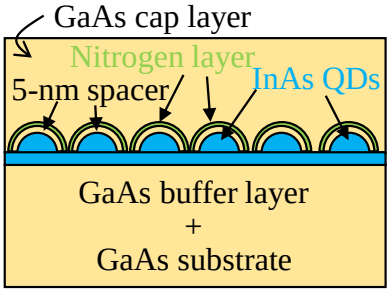

Fig. 1. Image of sample structure. The NQD sample does not include the spacer layer.

The measurements of the THz waves were conducted at 297 K using a Ti:sapphire pulse laser having a pulse width of approximately 100 fs. The schematic diagram of the measurement system is shown in Fig. 2. The central energy of the laser pulse was changed from 1.653 eV to 1.425 eV. The pump density was maintained at 0.14 μJ/cm^2. The samples were excited by pump pulses at an approximately 45° incidence angle. The THz wave emitted from the samples was collected with a pair of off-axis parabolic mirrors and detected by a commercial photoconductive dipole antenna fabricated on a low-temperature-grown GaAs film (TERA8, Thorlabs). In the measurement of PL

OSA CONTINUUM

excitation spectra of QDs, the excitation light was produced by the combination of a fiber laser with a repetition rate of 20 MHz as the white light source and a 27-cm single monochromator with a resolution of 1.2 nm. The emitted light was dispersed by a 14-cm single monochromator with a resolution of 3 nm and was detected by an InGaAs diode array. Furthermore, for the measurement of the PL spectrum of the QDs and GaAs to clarify the formation of nitrogen-doped layer, a 34-cm single monochromator with a resolution of 0.3 nm and an InGaAs diode array were used.

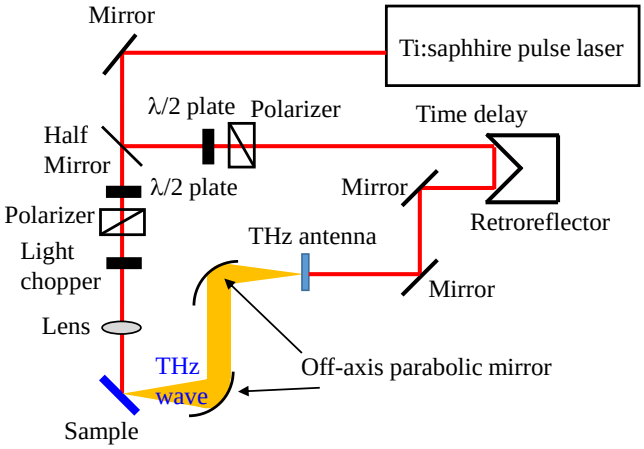

Fig. 2. Schematic diagram of the THz-wave measurement system.

3. Results and discussion

Figures 3(a) and 3(b) depict the time-domain THz signals measured at various pump energies for the NQD and NQD(5 nm) samples, respectively. In addition to the difference in the dependence of the amplitude on the excitation energy, both the samples showed phase inversion at different energies of 1.459 eV for NQD and 1.493 eV for NQD(5 nm). Considering that the phase inversion occurs at 1.459 eV in the reference QD [26], the energy of the phase inversion is observed to vary with the structure.

To clarify the energy of the phase inversion, the initial rise of signal ΔA, shown in Fig. 3(a), was plotted as a function of pump energy and is denoted using triangles and circles for NQD and NQD(5 nm) in Fig. 4, respectively. The horizontal dotted line indicates $\Delta A = 0$. The vertical dotted line demonstrates the phase inversion energy in the reference QD [26]. The phase inversion energies for the NQD and NQD(5 nm) samples shifted to the lower and higher energy sides when compared with the energy of reference QD, respectively.

Furthermore, covering QDs with nitrogen atoms also modified the dependence of the THz intensity. The Fourier transformation (FT) intensities in the samples are depicted in Fig. 5. The profile of the reference sample is also depicted [26]. As described in the previous report, numerical FT was performed for the signals in the time range from 1.5 ps to 4.0 ps. Because the signals were measured without purging, the free induction decay of the water vapor overlapped on the time-domain signal. This effect enhances the intensity of the high frequency component. Therefore, we focused on a peak intensity of approximately 0.8 THz. In Fig. 5, the FT peak intensities were plotted as a function of pump energy. The intensity values were normalized by the excitation photon number. The intensity in the reference QD sample, indicated by the closed circles, remained in the low pump-energy region. In contrast, the intensity profile of NQD, which is indicated by the triangles, gradually decreases toward the bandgap energy of GaAs, which is

OSA CONTINUUM

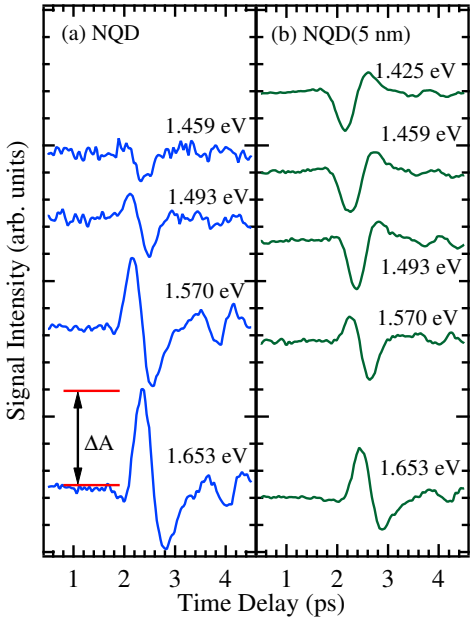

Fig. 3. Dependence of the THz signal on the pump energy for the (a) NQD and (b) NQD(5 nm) samples.

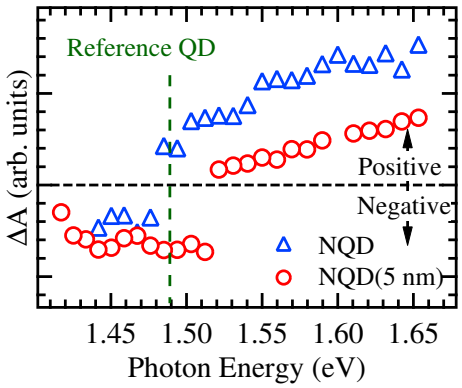

Fig. 4. Dependence of ΔA on the pump energy for the NQD and (b) NQD(5 nm) samples plotted using triangle and circles, respectively. The vertical dotted line indicates the phase inversion energy for the reference QD sample.

indicated by the downward allow. This indicates that the THz emission from the cap layer with a thickness of 150 nm becomes dominant in the NQD sample. Furthermore, the intensity profile of NQD(5 nm) seems to be unique. The intensity of more than 1.55 eV has a similar dependence to that of NQD, whereas it increases at less than 1.55 eV and is similar to the reference.

The PL spectrum does not indicate the origin of these changes. The PL and PL excitation spectra observed at the PL peak energy are depicted in Fig. 6. The dotted curves denote the PL spectra from the GaAs in each sample. The vertical arrows indicate the energy of phase inversion. The PL excitation spectra do not show any specific structure, resulting in THz signal phase inversion for all the samples. Upon only considering the PL intensity, peak energy, and decay time of the QDs, the NQD(5 nm) and reference QD samples are almost the same, whereas

OSA CONTINUUM

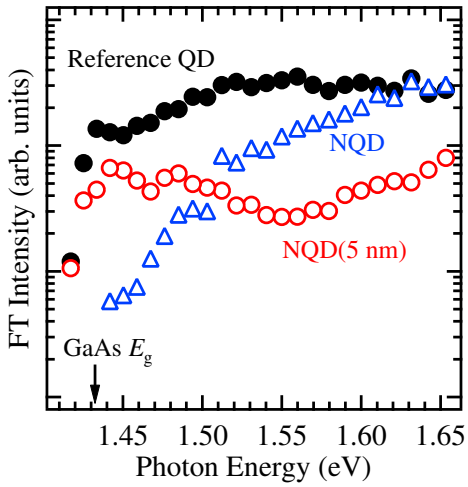

Fig. 5. The FT intensities for NQD and NQD(5 nm) plotted as a function of pump energy by triangles and open circles, respectively. The closed circles indicate the intensities obtained for the reference QD sample [26].

the NQD sample is different. However, the polarization property of the QDs in the NQD(5 nm) sample is different from that of other samples [20], suggesting that the strain distribution in the NQD(5 nm) sample is different and related to the difference in the phase inversion energy.

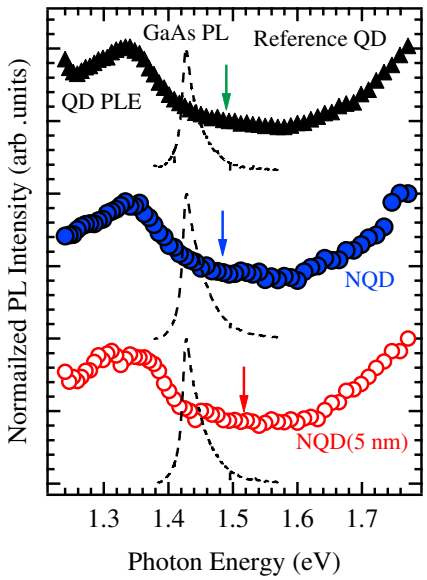

Fig. 6. The PL and PL excitation spectra of the reference QD, NQD, and NQD(5 nm) samples from top to bottom as denoted by dotted curves and marks, respectively. The arrows indicate the energy of the phase inversion of the THz signal.

The electronegativity of the nitrogen atom may be considered as the origin of the variation of the THz properties. In case of dilute doping of nitrogen atom into GaAs, the localized exciton luminescence, which is known as isoelectronic luminescence, was observed because the nitrogen atom attracted electrons [28–31]. Namely, the electron diffusion toward the surface direction

OSA CONTINUUM

causes the phase inversion because the nitrogen atom attracts the electrons generated in the bottom layer. However, the attractive force does not depend on the excitation energy. Therefore, the effect of electronegativity on phase inversion is considerably less.

Furthermore, the possibility of shift current was considered [32,33]. In case of the shift current, the phase depends on the pump energy; the phase change has been observed by the excitation of the heavy-hole and light-hole excitons in previous studies. However, as mentioned above, there is no specific state around the energy of phase inversion. Therefore, the possibility of the shift current was barely considered.

The difference in THz properties originates from the formation of a thin GaNAs layer. To show the formation of the GaNAs layer, the PL spectra were measured at a high excitation power. In Fig. 7, the PL spectra of the samples that are measured at room temperature are depicted. The dotted and solid curves indicate the spectra measured under low (20 mW) and high (150 mW) excitation conditions, respectively. Reference QD denotes the exciton peaks including the high state transition, as denoted by the downward closed triangles. On the other hand, the spectra for the samples that include the nitrogen layer denote additional broad peaks between the QDs and GaAs, as indicated by the open downward triangles, and the PL energies almost agree with those of the δ nitrogen-doped GaAs [34,35]. Because of negative bowing, although the lattice constant of GaNAs is smaller than that of GaAs, the bandgap energy of GaNAs is smaller than that of GaAs [36,37]. Therefore, the additional peaks are attributed to the formation of the GaNAs layer. By considering the time of nitridation to remain the same the difference between the peak energies for the two samples originated from the nitridation temperature. In case of the NQD sample, the nitrogen atoms were added at 400°C, whereas the temperature for the NQD(5 nm) sample was 450°C.

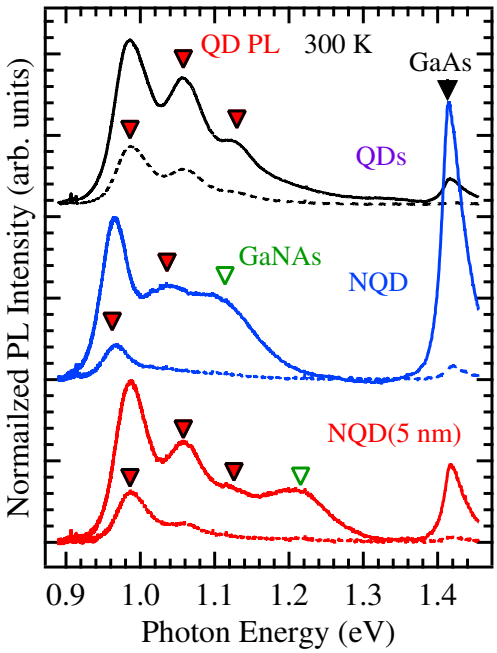

Fig. 7. The PL spectra measured for different excitation intensities; the dashed and the solid curves represent the low and high excitation densities, respectively. A continuous laser was used.

Furthermore, the strain also changed the transition energy of the GaNAs layer. In the NQD sample, the nitrogen atoms were directly added on the InAs QDs; the lattice constant was

OSA CONTINUUM

modified by both InAs and GaAs. Because of the large binding energy of the In-N bonding, In segregation was suppressed, which lowers the PL energy from GaNAs layer due to the large strain. On the other hand, the lattice constant for the NQD(5 nm) sample was only modified by GaAs. Therefore, the lattice constant for the NQD(5 nm) sample was smaller than that for the NQD sample. By considering the distribution of strain and phase inversion of the THz signal, the nitrogen layer produces a strong strain field to the underneath layer, in particular, for the layer between the GaAs spacer and the QD layer. From this result, it can be said that InAs QDs works as one of the strain buffer layers.

4. Conlcusion

We have investigated the variation of the THz signals that were observed at various pump energies for samples that included InAs QDs with a nitrogen-doped layer. The phase of the transient THz signal changed with the sample structure; in comparson with the reference QD sample, the phase inversion energy shifted to the lower and higher energy sides of the NQD and NQD(5 nm) samples, respectively. Although the QD PL peak energies for the reference QD and NQD(5 nm) were almost the same, the potential structure around the QDs exhibited a considerable change. The formation of a dilute nitrogen-doped layer is the origin of this change which is caused by several factors including the change of the lattice constants and In segregation. Our results will lead to improved performance of the QD optical devices, for example, for carrier injection by changing the work function of the electrode. In addition, enhancement of the non-radiative relaxation of carriers due to modification of the potential can be used for the ultrafast optical device application. Furthermore, the extension of the THz wave emission energy to the lower energy side suggest that the QDs with the spacer layer may be used for the THz photoconductive antenna.

Funding

Japan Society for the Promotion of Science (JSPS) (16KK0129, JP26289088); Research Foundation for the Electrotechnology of Chubu.

References

1. M. A. Majid, D. T. D. Childs, K. Kennedy, R. Airey, R. A. Hogg, E. Clarke, P. Spencer, and R. Murray, "O-band excited state quantum dot bilayer lasers," Appl. Phys. Lett. **99**(5), 051101 (2011).
2. C. Liu, H. Wang, Q. Meng, B. Gao, and K. S. Ang, "Modal gain and photoluminescence investigation of two-state lasing in GaAs-based 1.3 μm InAs/InGaAs quantum dot lasers," Appl. Phys. Express **6**(10), 102702 (2013).
3. K. Akahane, N. Yamamoto, A. Kanno, K. Inagaki, T. Umezawa, T. Kawanishi, T. Endo, Y. Tomomatsu, and T. Yamanoi, "Stable two-mode emission from semiconductor quantum dot laser," Appl. Phys. Express **6**(10), 104001 (2013).
4. V. B. Verma, M. J. Stevens, K. L. Silverman, N. L. Dias, A. Garg, J. J. Coleman, and R. P. Mirin, "Photon antibunching from a single lithographically defined InGaAs/GaAs quantum dot," Opt. Express **19**(5), 4182 (2011).
5. C. Schneider, T. Heindel, A. Huggenberger, T. A. Niederstrasser, S. Reitzenstein, A. Forchel, Höfling, and M. Kamp, "Microcavity enhanced single photon emission from an electrically driven site-controlled quantum dot," Appl. Phys. Lett. **100**(9), 091108 (2012).
6. Y.-M. He, Y. He, Y.-J. Wei, D. Wu, M. Atatüre, C. Schneider, S. Höfling, M. Kamp, C.-Y. Lu, and J.-W. Pan, "On-demand semiconductor single-photon source with near-unity indistinguishability," Nat. Nanotechnol. **8**(3), 213–217 (2013).
7. D. Zhou, G. Sharma, S. F. Thomassen, T. W. Reenaas, and B. O. Fimland, "Optimization towards high density quantum dots for intermediate band solar cells grown by molecular beam epitaxy," Appl. Phys. Lett. **96**(6), 061913 (2010).
8. D. Guimard, R. Morihara, D. Bordel, K. Tanabe, Y. Wakayama, M. Nishioka, and Y. Arakawa, "Fabrication of InAs/GaAs quantum dot solar cells with enhanced photocurrent and without degradation of open circuit voltage," Appl. Phys. Lett. **96**(20), 203507 (2010).
9. S. Asahi, H. Teranishi, K. Kusaki, T. Kaizu, and T. Kita, "Two-step photon up-conversion solar cells," Nat. Commun. **8**, 14962 (2017).
10. J. Persson, U. Håkanson, M. K.-J. Johansson, L. Samuelson, and M.-E. Pistol, "Strain effects on individual quantum dots: Dependence of cap layer thickness," Phys. Rev. B **72**(8), 085302 (2005).

OSA CONTINUUM

11. K. Akahane, N. Yamamoto, S. Gozu, and N. Ohtani, "Strong photoluminescence and laser operation of InAs quantum dots covered by a GaAsSb strain-reducing layer," Phys. E **26**(1-4), 395–399 (2005).
12. V. V. Chaldyshev, N. A. Bert, A. L. Kolesnikova, and A. E. Romanov, "Stress relaxation scenario for buried quantum dots," Phys. Rev. B **79**(23), 233304 (2009).
13. O. Brandt, L. Tapfer, K. Ploog, R. Bierwolf, and M. Hohenstein, "Effect of In segregation on the structural and optical properties of ultrathin InAs films in GaAs," Appl. Phys. Lett. **61**(23), 2814–2816 (1992).
14. T. Walther, A. G. Cullis, D. J. Norris, and M. Hopkinson, "Nature of the Stranski-Krastanow transition during epitaxy of InGaAs on GaAs," Phys. Rev. Lett. **86**(11), 2381–2384 (2001).
15. T. Kaizu, T. Matsumura, and T. Kita, "Broadband control of emission wavelength of InAs/GaAs quantum dots by GaAs capping temperature," J. Appl. Phys. **118**(15), 154301 (2015).
16. T. Kita, Y. Masuda, T. Mori, and O. Wada, "Long-wavelength emission from nitridized InAs quantum dots," Appl. Phys. Lett. **83**(20), 4152–4153 (2003).
17. O. Schumann, L. Geelhaar, H. Riechert, H. Cerva, and G. Abstreiter, "Morphology and optical properties of InAs(N) quantum dots," J. Appl. Phys. **96**(5), 2832–2840 (2004).
18. T. Kita, T. Mori, H. Seki, M. Matsushita, M. Kikuno, O. Wada, H. Ebe, M. Sugawara, Y. Arakawa, and Y. Nakata, "Extended wavelength emission to 1.3 μm in nitrided InAs/GaAs self-assembled quantum dots," J. Appl. Phys. **97**(2), 024306 (2005).
19. Y. D. Jang, N. J. Kim, J. S. Yim, D. Lee, S. H. Pyun, W. G. Jeong, and J. W. Jang, "Strong photoluminescence at 1.3 μm with a narrow linewidth from nitridized InAs/GaAs quantum dots," Appl. Phys. Lett. **88**(23), 231907 (2006).
20. T. Inoue, M. Mamizuka, H. Mizuno, O. Kojima, T. Kita, and O. Wada, "Effects of indium segregation on optical properties of nitrogen-doped InAs/GaAs quantum dots," J. Appl. Phys. **104**(10), 103532 (2008).
21. M. Strauss, S. Höfling, and A. Forchel, "InAs/GaInAs(N) quantum dots on GaAs substrate for single photon emitters above 1300 nm," Nanotechnology **20**(50), 505601 (2009).
22. D. Birkedal, O. Hansen, C. B. Sørensen, K. Jarasiunas, S. D. Brorson, and S. R. Keiding, "Terahertz radiation from delta-doped GaAs," Appl. Phys. Lett. **65**(1), 79–81 (1994).
23. M. B. Johnston, D. M. Whittaker, A. Corchia, A. G. Davies, and E. H. Linfield, "Simulation of terahertz generation at semiconductor surfaces," Phys. Rev. B **65**(16), 165301 (2002).
24. J. Lloyd-Hughes, S. K. E. Merchant, L. Fu, H. H. Tan, C. Jagadish, E. Castro-Camus, and M. B. Johnston, "Influence of surface passivation on ultrafast carrier dynamics and terahertz radiation generation in GaAs," Appl. Phys. Lett. **89**(23), 232102 (2006).
25. D. McBryde, M. E. Barnes, S. A. Berry, P. Gow, H. E. Beere, D. A. Ritchie, and V. Apostolopoulos, "Fluence and polarisation dependence of GaAs based Lateral Photo-Dember terahertz emitters," Opt. Express **22**(3), 3234–3243 (2014).
26. O. Kojima, R. Izumi, and T. Kita, "Effect of lattice-mismatch strain on electron dynamics in InAs/GaAs quantum dots as seen by time-domain terahertz spectroscopy," J. Phys. D: Appl. Phys. **51**(30), 305102 (2018).
27. M. Mamizuka, O. Kojima, T. Inoue, T. Kita, and O. Wada, "Exciton response controlled by introducing a spacer layer in nitrided InAs quantum dots," Phys. Status Solidi C **6**(S1), S146–S149 (2018).
28. X. Liu, M.-E. Pistol, and L. Samuelson, "Excitons bound to nitrogen pairs in GaAs," Phys. Rev. B **42**(12), 7504–7512 (1990).
29. S. Francoeur, S. A. Nikishin, C. Jin, Y. Qiu, and H. Temkin, "Excitons bound to nitrogen clusters in GaAsN," Appl. Phys. Lett. **75**(11), 1538–1540 (1999).
30. T. Kita and O. Wada, "Bound exciton states of isoelectronic centers in GaAs:N grown by an atomically controlled doping technique," Phys. Rev. B **74**(3), 035213 (2006).
31. T. Kita, Y. Harada, and O. Wada, "Fine structure splitting of isoelectronic bound excitons in nitrogen-doped GaAs," Phys. Rev. B **77**(19), 193102 (2008).
32. M. Bieler, K. Pierz, U. Siegner, and P. Dawson, "Shift currents from symmetry reduction and Coulomb effects in (110)-orientated GaAs/$Al_{0.3}Ga_{0.7}$As quantum wells," Phys. Rev. B **76**(16), 161304 (2007).
33. S. Priyadarshi, M. Leidinger, K. Pierz, A. M. Racu, U. Siegner, M. Bieler, and P. Dawson, "Terahertz spectroscopy of shift currents resulting from asymmetric (110)-oriented GaAs/AlGaAs quantum wells," Appl. Phys. Lett. **95**(15), 151110 (2009).
34. F. Ishikawa, S. Furuse, K. Sumiya, A. Kinoshita, and M. Morifuji, "Nitrogen δ-doping for band engineering of GaAs-related quantum structures," J. Appl. Phys. **111**(5), 053512 (2012).
35. Y. Ogawa, Y. Harada, T. Baba, T. Kaizu, and T. Kita, "Effects of rapid thermal annealing on two-dimensional delocalized electronic states of the epitaxial N δ-doped layer in GaAs," Appl. Phys. Lett. **108**(11), 111905 (2016).
36. W. Shan, K. M. Yu, W. Walukiewicz, and J. W. Ager III, "Reduction of band-gap energy in GaNAs and AlGaNAs synthesized by N^+ implantation," Appl. Phys. Lett. **75**(10), 1410–1412 (1999).
37. K. Matsuda, T. Saiki, M. Takahashi, A. Moto, and S. Takagishi, "Near-field photoluminescence study of GaNAs alloy epilayer at room and cryogenic temperature," Appl. Phys. Lett. **78**(11), 1508–1510 (2001).